ELSEVIER

Polymer 43 (2002) 3571–3577

polymer

www.elsevier.com/locate/polymer

Photoinduced electron transfer in nanostructures of ultrathin polyimide films containing porphyrin moieties

Hideo Ohkita, Takeo Ogi, Ryoji Kinoshita, Shinzaburo Ito*, Masahide Yamamoto[1]

Department of Polymer Chemistry, Graduate School of Engineering, Kyoto University, Yoshida, Sakyo-ku, Kyoto 606-8501, Japan

Dedicated to Professor Imanishi on the occasion of his retirement

Received 7 December 2001; received in revised form 4 February 2002; accepted 20 February 2002

Abstract

Photoinduced electron transfer between porphyrin moieties and pyromellitimide fragments has been investigated in multi-layered structures of ultrathin polyimide films prepared by the Langmuir–Blodgett (LB) technique. The LB films were composed of three kinds of polyimides, which contained zinc tetraphenylporphyrin (ZnTPP) unit as an electron donor (D-layer), no chromophoric groups (S-layer), and pyromellitimide fragments as an electron acceptor (A-layer). The layered structure and orientational distribution of porphyrin moieties in the LB films were evaluated by surface plasmon measurement and absorption dichroism measurement, respectively. The thickness of monolayer was estimated to be 0.9 nm for the polyamic acid films and 0.4 nm for the polyimide films. The molecular plane of porphyrin moieties was oriented in the direction parallel to the substrate plane. In the multi-layered structures of polyimide LB films, the efficiencies of photoinduced electron transfer from porphyrin moieties to pyromellitimide fragments varied sharply with the number of spacing layers, indicating that the short-range interactions such as electron transfer could be controlled by the fabric of ultrathin films. The rate of electron transfer observed by the fluorescence quenching measurements was numerically simulated for the nanostructure using the Monte Carlo method.

Keywords: Polyimide Langmuir–Blodgett film; Porphyrin; Photoinduced electron transfer

1. Introduction

The Langmuir–Blodgett (LB) method is one of the most powerful techniques for constructing layered nanostructures. Historically, Kuhn and his coworkers demonstrated that the designed nanostructures of fatty acid LB films can control elemental photophysical processes such as excitation energy transfer and electron transfer [1–3]. Fujihira et al. reported an electrochemical photodiode consisting of LB films on electrodes where the photoinitiated vectorial flow of electrons can be achieved [4–6]. Polymer LB films have many advantages compared with the LB films consisting of fatty acids with long alkyl chains [7–12]. Among them, the absence of long alkyl chains in polymer LB films enables us to construct more thin layered-structures in a scale of nanometers. Our research group has studied excitation energy transfer [13–15] and two-photon ionization [16,17] in multi-layered structures of ultrathin polymer films where the distance between donor and acceptor molecules can be controlled in a nanometer-scale precision. The energy transfer based on the Förster mechanism and the photoionization will occur in a spatial scale from one nanometer to several nanometers. On the other hand, photoinduced electron transfer between isolated donor and acceptor molecules will typically occur in a scale of 1–2 nm [18]. Therefore, the molecular design in a scale of <1 nm is crucially required to control the photoinduced electron transfer between donor and acceptor molecules.

Mimicking natural photosynthetic reaction centers where orientation and placement of the chromophores are well organized in a scale of <1 nm [19], many researchers have designed and synthesized elegant intramolecular donor–acceptor system having porphyrin moieties [20]. Osuka and his coworkers synthesized diporphyrin–porphyrin–pyromellitimide triads and demonstrated that a sequential electron transfer relay in the triads resembles that in the reaction center and results in the formation of long-lived charge separation state [21]. Gust and Moore synthesized cartenoid–porphyrin–quinone triads and not only made a light-driven transmembrane proton pump but also synthesized ATP in a lipid bilayer membrane incorporated

* Corresponding author. Tel.: +81-75-753-5602; fax: +81-75-753-5632.
E-mail address: sito@polym.kyoto-u.ac.jp (S. Ito).
[1] Present address: Faculty of Science and Engineering, Ritsumeikan University, Kusatsu, Shiga 525-8577, Japan.

0032-3861/02/$ - see front matter
PII: S0032-3861(02)00160-X

with the triad, quinone, and CF_0F_1-ATP synthase [22]. Imahori and his coworkers reported highly efficient photovoltaic cells consisting of gold electrodes modified with a self-assembled monolayer of ferrocene–porphyrin–C_{60} triad [23]. These successful researches are the fruits of artful synthetic techniques.

Our approach is not based on these synthetic techniques but on the fabrication techniques with ultrathin polymer films. To keep the distance between donor and acceptor molecules in a scale of <1 nm, we used polyimide LB films with a thickness reported to be only 0.40–0.56 nm [24]. Here, we prepared three kinds of polyimides, one each used as an electron donor layer (D), a spacing layer (S), and an electron accepting layer (A). The D-layer had zinc tetraphenylporphyrin (ZnTPP) unit as an electron donor, and the A-layer had pyromellitimide fragments as an electron acceptor. The layered structure and orientational distribution of porphyrin moieties in the LB films were evaluated by surface plasmon measurement and absorption dichroism measurement, respectively. In the layered structure, the distance between the porphyrin moieties and pyromellitimide fragments was controlled in a scale of 1 nm by changing the number of spacing layers. Using the multilayered polyimide films, we successfully controlled the photoinduced electron transfer from porphyrin moieties in the excited state to pyromellitimide fragments and studied the distance dependence by comparison with a numerical simulation based on the Monte Carlo method.

2. Experimental section

2.1. Materials

2.1.1. ZnDATPPs

Diamino-tetraphenylporphyrin (DATPP), a mixture of 5,10-bis(4-aminophenyl)-15,20-diphenyl-21*H*,23*H*-porphine (*cis*-DATPP) and 5,15-bis(4-aminophenyl)-10,20-diphenyl-21*H*,23*H*-porphine (*trans*-DATPP), was synthesized by the reactions of *p*-nitrobenzaldehyde (Nacalai Tesque), benzaldehyde (Nacalai Tesque), and pyrrole (Wako Pure Chemical Industries, Ltd.) as starting reactants, in accordance with the method of Kakimoto et al. [25]. To a solution of 30 ml of THF was added 101.3 mg of DATPP and 202.7 mg of zinc acetylacetonate hydrate. The solution was refluxed for 4 h, cooled to room temperature, and then the solvent was evaporated. The precipitate was partly dissolved in a methanol solution by heating and left overnight at 0 °C. The resulting violet crystals were collected, washed with methanol, and then dried to afford ZnDATPP.

2.1.2. Polyamic acids

Three kinds of polyamic acids were synthesized as a precursor of polyimides as shown in Fig. 1. The donor polyamic acid was synthesized by the reaction of 4,4′-oxydiphthalic anhydride (ODPA) (5 mmol), 4,4′-oxydianiline (ODA) (4.9 mmol), and ZnDATPP (0.1 mmol); spacer polyamic acid synthesized by the reaction of ODPA and ODA; acceptor polyamic acid synthesized by the reaction of pyromellitic dianhydride (PMDA) and ODA. To a solution of 5 mmol of diamine monomer in dried *N*,*N*-dimethylacetamide (DMA) was added equivalent of tetracarboxylic anhydrides in a drybox. The solution was stirred at room temperature until the viscosity increased. The polyamic acids obtained were stored at −15 °C.

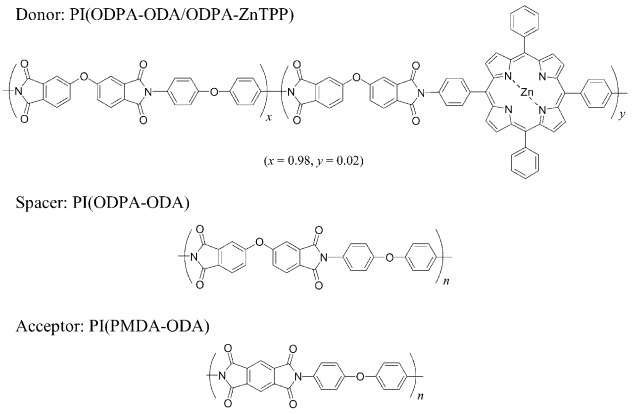

Fig. 1. Three kinds of polyimide used in this study: PI(ODPA–ODA/ODPA–ZnTPP) used as an electron donor (D) has a zinc tetraphenylporphyrin unit, PI(ODPA–ODA) used as a spacer (S) has no chromophoric groups, PI(PMDA–ODA) used as an electron acceptor (A) has pyromellitimide groups. The mole fraction of ZnTPP moieties was 2 mol%. The ZnTPP-containing unit consisted of a mixture of *trans*-ZnTPP and *cis*-ZnTPP.

2.1.3. Other materials

5,10,15,20-Tetraphenyl-21*H*,23*H*-porphine zinc (ZnTPP) and pyromelltic diimide (PMDI) were purchased from Aldrich Chem. Co., Inc. Polystyrene (Scientific Polym. Prod., Inc.) was purified by reprecipitation from a benzene solution to methanol three times.

2.2. Sample preparation

Polyamic acid LB films were prepared in accordance with the procedure of Kakimoto et al. [25]. The benzene–DMA (1:1) solution of polyamic acid salt with *N*,*N*-dimethylhexadecylamine was spread on water in a trough (Kenkosha model SI-1) with a Wilhelmy-type film balance. The polyamic acid was deposited on a quartz plate (10×40 mm^2) at a temperature of 10 °C, a surface pressure of 12.5 mN m^{-1}, and a dipping speed of 10 mm min^{-1}. The first layer was deposited as a Z-type LB film and the following layers as a Y-type LB film with a high transfer ratio both in the up and down modes. The water in the subphase was purified by deionization, distillation, and passing through a filtration system (Barnstead Nanopure II). The quartz plates used as a substrate were cleaned in an oxidative sulfuric acid solution and rinsed with water several times. The polyamic acid films were dried overnight in a desiccator and then

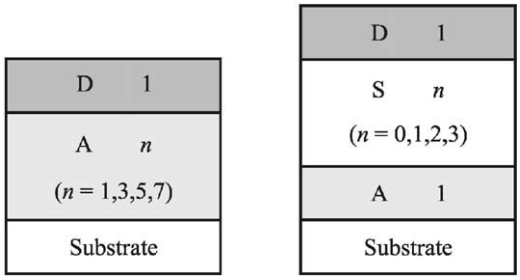

Fig. 2. Multi-layered structures of polyimide LB films: (left) DA*n* consists of one D-layer and *n* A-layers; (right) DS*n*A consists of one D-layer, *n* S-layers, and one A-layer on a quartz substrate.

immersed in a mixture of acetonitrile–acetic anhydride–pyridine (30:1:1) for 2 h, yielding polyimide LB films. Fig. 2 shows the layered structures of polyimide LB films. The DA*n* and DS*n*A were fabricated on the quartz plate in the following sequence:

DA*n*

1. *n* (= 1, 3, 5, 7) layers of PI(PMDA–ODA) as the electron-accepting layers (A-layer);
2. one layer of PI(ODPA–ODA/ODPA–ZnTPP) as the electron-donating layer (D-layer).

DS*n*A

1. one layer of PI(PMDA–ODA) as the electron-accepting layers;
2. *n* (= 0, 1, 2, 3) layers of PI(ODPA–ODA) as the spacing layers (S-layer);
3. one layer of PI(ODPA–ODA/ODPA–ZnTPP) as the electron-donating layer.

For the Perrin analysis, polystyrene films doped with ZnTPP and PMDI were prepared by the spin-casting method: the dopant chromophores were dissolved in a chlorobenzene solvent with the polystyrene. More than two films were prepared under the same condition to average the fluorescence intensity.

2.3. Measurements

Fluorescence spectra were measured with a fluorescence spectrophotometer (Hitachi, 850). Infrared absorption spectra were measured with an FT-IR spectrometer (Perkin Elmer, System-2000). Ultraviolet–visible absorption spectra were measured with a spectrophotometer (Hitachi, U-3500). For the evaluation of the orientation of porphyrin moieties in LB films, the absorbances were measured for the vertically or horizontally polarized light through a Glan–Thompson ultraviolet prism polarizer (Karl Lambrecht) attached to the spectrophotometer [26]. Fig. 3 shows optical alignment of the absorption dichroism measurement. Fluorescence decay was measured by the time-correlated single photon counting method. Details of the time-resolved measurement have been described elsewhere [27].

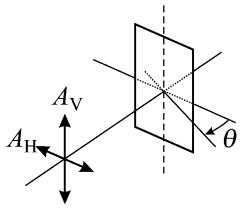

Fig. 3. Optical systems for the absorption dichroism measurements. The A_V and A_H represent absorbance for vertically and horizontally polarized light, respectively. The angle θ is a tilting angle between the direction of incident light and the direction normal to the quartz substrate.

3. Results and discussion

3.1. Structure of polyamic acid and polyimide LB films

In this study, the ether type anhydrate (ODPA) and diimide (ODA) were employed as the monomer units of polyimide. This is because these are electronically inert for the donor and the acceptor even in the excited states, therefore, the electronic interactions of chromophores could be selectively observed in the condensed matrices of polyimide. However, the polyamic acid obtained was soluble in benzene, which is one component of chemicals for the imidization reaction and tends to break the layered structure of the polyamic acid. Acetonitrile was found to be a good solvent enough to replace benzene. First, we evaluate the layered structure of polyamic acid and polyimide LB films before and after imidization reaction by the surface plasmon measurement. The reaction was monitored by the FT-IR measurement for LB films deposited on silicon wafers. After the treatment, the absorption bands due to the alkylamine chains (2920, 2850 cm^{-1}) disappeared whereas the absorption bands due to the carbonyl groups of imide units (1720 cm^{-1}) appeared.

Fig. 4 shows surface plasmon curves of polyamic acid LB films deposited on a quartz plate covered with 50 nm thick gold. The resonance peaks shifted to higher angles with increases in the number of layers. This peak shift clearly shows the increase in thickness of the LB films, which can be evaluated quantitatively by the fitting analysis using the Fresnel's equation [28].[2] Fig. 5 shows dependence of the thickness of the polyamic acid (closed circle) and polyimide (open triangle) films, before and after the chemical treatment of imidization. The thickness linearly increased for both polyamic acid and polyimide LB films as a function of the number of layers. These linear increases prove that each polyamic acid and polyimide layer was well deposited layer-by-layer and was not peeled off during the treatment. The thickness was estimated to be 0.9 nm for the polyamic acid monolayer and 0.4 nm for the polyimide monolayer

[2] The refractive index was found to be 1.577 for polyamic acid films and 1.590 for polyimide films by the total reflection method. In the surface plasmon analysis, we used these values as the refractive index for each polymer LB film.

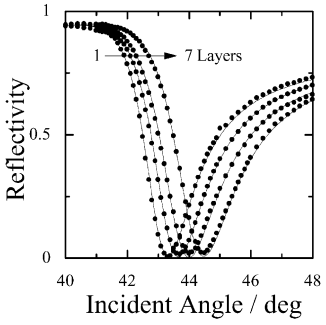

Fig. 4. Surface plasmon plots of polyamic acid alkylamine salt LB films: from left to right, 1, 3, 5, 7 layers on a quartz plate with 50 nm thick gold. Solid curves are fitting results using the Fresnel's equation. Refractive index of the polymer LB films was fixed to 1.577 for polyamic acid alkylamine salt and to 1.590 for polyimide, which were determined by the total reflection method.

from the slope in Fig. 5. The decrease in the thickness after the treatment was due to the elimination of long alkylamine chain by the imidization reaction. These findings show that both polyamic acid and polyimide LB films retain the multilayered structure before and after the imidization treatment and that the ultrathin polyimide films enable one to construct a layered nanostructure in a scale of <1 nm.

Next, we evaluated the orientation of porphyrin moieties in polyamic acid and polyimide LB films before and after the imidization reaction by absorption dichroism measurement. The absorbance at a tilting angle of θ for the vertically polarized light $A_{\theta V}$ depends on only optical path length and is independent of the orientational distribution of molecules. On the other hand, the absorbance at a tilting angle of θ for the horizontally polarized light $A_{\theta H}$ depends on the orientational distribution of molecules. Therefore, theoretical calculation predicts that the absorbance ratios of $A_{\theta V}/A_{0V}$ to $A_{\theta H}/A_{0H}$ should be $(\cos\theta)^{-2}$ for two-dimensional orientation of porphyrin moieties in the substrate plane and should be unity for three-dimensional orientation of porphyrin moieties in the LB films. Fig. 6 shows the absorbance ratios of $A_{\theta V}/A_{0V}$ to $A_{\theta H}/A_{0H}$ for polyamic acid and polyimide LB films containing porphyrin moieties as a function of titling angles.

Both absorbance ratios for polyamic acid and polyimide

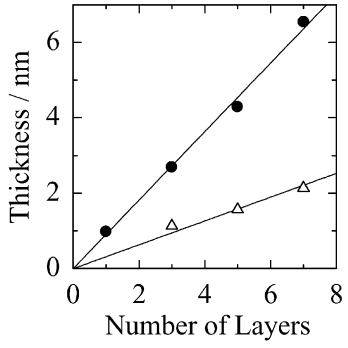

Fig. 5. Dependence of the thickness evaluated from the surface plasmon measurement on the number of layers: polyamic acid alkylamine salt LB films (closed circle) and polyimide LB films (open triangle).

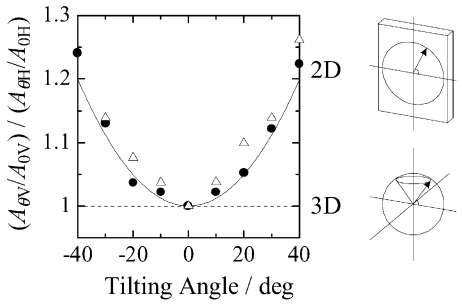

Fig. 6. Absorbance ratio of $A_{\theta V}/A_{0V}$ to $A_{\theta H}/A_{0H}$ measured at Soret bands of porphyrin moieties as a function of tilting angles θ: 20 layers of polyamic acid (closed circle) and polyimide (open triangle) LB films containing porphyrin moieties. The angle θ is corrected by the refractive index of polyamic acid ($n = 1.577$). Solid curve and broken line show the theoretical prediction for two-dimensional orientation and for three-dimensional orientation, respectively.

LB films containing porphyrin moieties were in agreement with the theoretical prediction for two-dimensional orientation of porphyrin moieties on the substrate plane. This orientation was the same as that of diimide fragments in polyimide LB films as previously reported [26]. Therefore, both porphyrin moieties and diimide fragments in the LB films are oriented on the two-dimensional plane before and after the imidization treatment.

3.2. Photoinduced electron transfer between porphyrin and imide groups in the LB films

First, we examined the electron-accepting ability of diimide fragments in polyamic acid and polyimide films by the fluorescence decay measurement of ZnTPP moieties in two kinds of LB films (D2S5 and D2A5 films). The D2S5 film consisted of two D-layers (ODPA–ODA/ODPA–ZnTPP) and five S-layers (ODPA–ODA) on a quartz substrate and the D2A5 film consisted of two D-layers (ODPA–ODA/ODPA–ZnTPP) and five A-layers (PMDA–ODA) on a quartz substrate. Fluorescence lifetimes were evaluated from the fitting analysis of the fluorescence decay by the non-linear least-squares method. The fluorescence decay $I(t)$ was fitted to a sum of three exponentials: $I(t) = A_1 \exp(-t/\tau_1) + A_2 \exp(-t/\tau_2) + A_3 \exp(-t/\tau_3)$. The fluorescence lifetime $\langle\tau\rangle$ was averaged by the following equation: $\langle\tau\rangle = \sum A_i\tau_i / \sum A_i$. The averaged fluorescence lifetime of ZnTPP moieties on S-layers in D2S5 films was about 1.5 ns before and after the imidization treatment. On the other hand, the averaged fluorescence lifetime of ZnTPP moieties on A-layers in D2A5 films was about 0.5 ns after the imidization whereas the lifetime was about 1.5 ns before the imidization. The averaged fluorescence lifetime of ZnTPP doped in polystyrene films without acceptor molecules was about 1.5 ns. Therefore, it is safely said that the fluorescence of ZnTPP moieties was quenched only by A-layers after the imidization and not quenched by S-layers before and after the imidization. These results show that pyromellitimide fragments in

PI(PMDA–ODA) have an electron-accepting ability whereas that of the diimide fragments in PI(ODPA–DA) have no electron-accepting ability. The electron-accepting ability is different probably because the conjugation of the diimide fragment in PI(ODPA–ODA) is lower than that in PI(PMDA–ODA) [29]. Therefore, PI(ODPA–ODA) is useful for adjusting the separation distance between the donor and acceptors with a thickness of only 0.4 nm.

Next, we evaluated the reaction radius and the rate constant of photoinduced electron transfer between ZnTPP and PMDI molecules from the comparison of the fluorescence quenching experiment with a numerical calculation based on the Monte Carlo method. The fluorescence intensity of ZnTPP with PMDI doped in polystyrene films decreased as the concentration of PMDI increased. Here we simulate the dependence of the fluorescence intensity of ZnTPP on the concentration of PMDI by the following Monte Carlo method [30].

As shown in Fig. 7, a donor molecule (ZnTPP) is located at the center of a $30 \times 30 \times 30\ \mathrm{nm}^3$ cubic space. Acceptor molecules (PMDI) are randomly located within the cubic space. The number of acceptor molecules corresponds to the acceptor concentration C_A ranging from 0 to $6.5 \times 10^{-2}\ \mathrm{nm}^{-3}$. The sum of electron transfer rate between an arbitrary donor i and all acceptors is calculated by Eq. (1) where r_{ij} is the distance between donor i and acceptor j; r_D and r_A are the radius of ZnTPP (0.43 nm) and PMDI (0.38 nm), respectively.

$$k_{ETi} = k_0 \sum_j \exp[-\beta(r_{ij} - (r_D + r_A))] \tag{1}$$

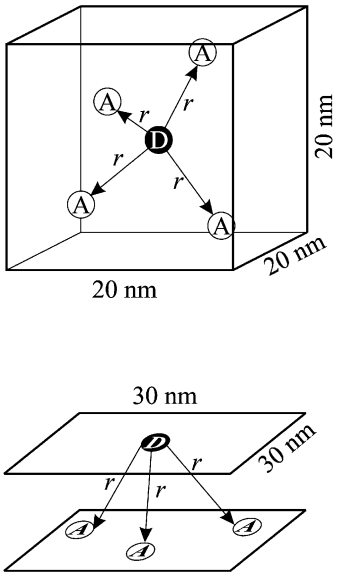

Fig. 7. Schematic illustration of the spatial distribution of chromophores used for the Monte Carlo simulation: top is three-dimensional model where a porphyrin donor molecule is located at a center of the cubic ($20 \times 20 \times 20\ \mathrm{nm}^3$) and acceptor molecules are randomly located within the cubic; bottom is two-dimensional model where a porphyrin donor molecule is located at a center of the D-layer plane ($30 \times 30\ \mathrm{nm}^2$) and acceptor molecules are randomly located within other A-layer planes.

The fluorescence decay of the donor i with acceptors is given by Eq. (2).

$$I_i(t) = I(0)\exp(-t/\tau_0 - k_{ETi}t) \tag{2}$$

Since the fluorescence decay observed $I(t)$ is the average of $I_i(t)$ for all donors (n_D molecules), $I(t)$ is calculated by Eq. (3).

$$I(t) = \frac{1}{n_D}\sum_i I_i(t) \tag{3}$$

Thus, the fluorescence intensity I in a steady state can be obtained from the integration of Eq. (3) from 0 to infinity with respect to time t.

$$I = \int_0^\infty I(t)\mathrm{d}t = \frac{I(0)}{n_D}\int_0^\infty \sum_i \exp(-t/\tau_0 - k_{ETi}t)\mathrm{d}t \tag{4}$$

In the same way, the fluorescence intensity I_0 in a steady state without any acceptors is given by Eq. (5).

$$I_0 = \frac{I(0)}{n_D}\int_0^\infty \sum_i \exp(-t/\tau_0)\mathrm{d}t = I(0)\tau_0 \tag{5}$$

Therefore, the intensity ratio can be calculated by Eq. (6).

$$\frac{I_0}{I} = n_D\tau_0\left(\int_0^\infty \sum_i \exp(-t/\tau_0 - k_{ET_i}t)\mathrm{d}t\right)^{-1} \tag{6}$$

According to the above procedure, we numerically calculated the intensity ratio I_0/I by the Monte Carlo method with various combinations of k_0 and β. Fig. 8 is the logarithmic plots of I_0/I versus concentration of PMDI. As shown in Fig. 8, which is called the Perrin plot, the experimental results (closed circles) were well reproduced by the numerical simulation with a combination of $k_0 = 5 \times 10^{12}\ \mathrm{s}^{-1}$ and $\beta = 9.1\ \mathrm{nm}^{-1}$ (open circles). The reaction radius of electron transfer between ZnTPP and PMDI was estimated to be about 1.7 nm from the slope of the solid line.

The parameters k_0 and β clearly show that electron transfer from porphyrin moieties in the excited state to pyromellitimide fragments is limited in a short distance range of around 1 nm: a distance parameter β of $9.1\ \mathrm{nm}^{-1}$ means that electron transfer rate decreases by a factor of 10^{-4} with

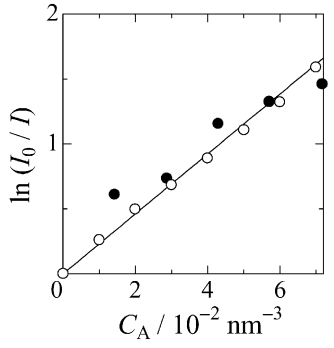

Fig. 8. Perrin plots of the ZnTPP fluorescence in polystyrene films doped with PMDI molecules: solid circles, fluorescence quenching experiments; open circles, numerical calculation by the Monte Carlo method.

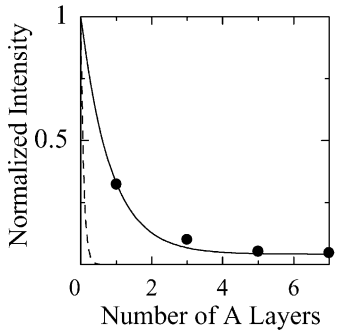

Fig. 9. Normalized fluorescence of the DA*n* LB films whose layered structure is shown in Fig. 2 (left). Solid and broken curves are obtained by the numerical calculation for the two-dimensional model with the 20% defects and without any defects, respectively.

a separation distance of 1 nm. Thus, nanostructures of the polyimide LB films having a thickness of 0.4 nm are suitable for controlling the electron transfer. Here, we show that photoinduced electron transfer from porphyrin moieties to pyromellitimide fragments can be controlled by the fabric of the polyimide LB films; the layered structures (DA*n* and DS*n*A) are shown in Fig. 2. As shown in Fig. 9, the fluorescence intensity of DA*n* films steeply decreased as the number of A-layers increased and was almost zero for more than two A-layers. On the other hand, as shown in Fig. 10, the fluorescence intensity of DS*n*A films increased as the number of S-layers increased and was almost unity for more than two S-layers. These fluorescence quenchings are not due to an excitation energy migration to quenching sites because the concentration of porphyrin moieties in the monolayer plane is so low that each porphyrin moiety is isolated. Thus, it is safely said that the fluorescence quenching was due to the electron transfer from the excited porphyrin moieties to the pyromellitimide and that the overall efficiencies were controlled by the separation distance between the donor and acceptor layers.

As shown in Figs. 9 and 10, the fluorescence quenching results (solid circles) were well reproduced by the numerical simulation (solid curve) with parameters of $k_0 = 5 \times 10^{12}\ s^{-1}$ and $\beta = 9.1\ nm^{-1}$ obtained from the Perrin analysis for the polystyrene bulk system. However, we have to introduce an assumption that surface coverage is 80% for each layer of the LB films. The residual 20% defects may result from the elimination of the long alkylamine chain on the way of imidization. In both Figs. 9 and 10, the solid and broken lines show the results of calculation with and without the defects, respectively. The actual system was well reproduced by the solid lines; on the other hand, the broken lines represent the characteristics of the electron transfer under the layered structure. The fluorescence of porphyrin moieties in D-layer was effectively quenched by only diimide fragments in the first and second layers from the D-layer. These findings clearly show that highly efficient electron transfers from the excited porphyrin moieties to pyromellitimide fragments and their artificial control can be achieved with multi-layered nanostructures of ultrathin polyimide films.

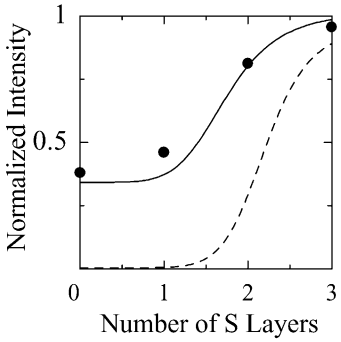

Fig. 10. Normalized fluorescence of the DS*n*A LB films whose layered structure is shown in Fig. 2 (right). Solid and broken curves are obtained by the numerical calculation for the two-dimensional model with the 20% defects and without any defects, respectively.

4. Conclusions

Multi-layered structures of LB films were prepared with three kinds of polyimides, i.e. a D-layer having ZnTPP unit as an electron donor, an S-layer having no chromophoric groups, and an A-layer having pyromellitimide fragments as an electron acceptor. The monolayer thickness was estimated to be 0.9 nm for polyamic acid LB films and 0.4 nm for polyimide LB films from the surface plasmon measurement. Porphyrin moieties in the LB films were distributed in the two-dimensional orientation in the direction parallel to the substrate plane. Fluorescence quenching of porphyrin moieties in the singlet excited state by pyromellitimide fragments was observed in the multi-layered polyimide LB films. The quenching results were numerically simulated on the basis of photoinduced electron transfer from porphyrin moieties. A good agreement was obtained showing that photoinduced electron transfer from porphyrin moieties in the singlet excited state to pyromellitimide fragments can be controlled in the multi-layered structure of polyimide films in which the distance between the porphyrin moieties and pyromellitimide fragments could be adjusted in a scale of <1 nm by changing the number of S-layers.

Acknowledgements

This work was supported by the Murata Science Foundation and the Takeda Science Foundation.

References

[1] Kuhn H. In: Weissberger A, Rossiter BW, editors. Physical methods of chemistry, vol. 1. New York: Wiley, 1972; part 3B.
[2] Möbius D. Ber Bunsenges Phys Chem 1978;82:848–58.
[3] Kuhn H. J Photochem 1979;10:111–32.

[4] Fujihira M, Nishiyama K, Yamada H. Thin Solid Films 1985;132:77–82.
[5] Nishikata Y, Morikawa A, Kakimoto M, Imai Y, Hirata Y, Nishiyama K, Fujihira M. J Chem Soc, Chem Commun 1989:1772–4.
[6] Nishikata Y, Fukui S, Kakimoto M, Imai Y, Nishiyama K, Fujihira M. Thin Solid Films 1992;210/211:296–8.
[7] Watanabe M, Kosaka Y, Oguchi K, Sanui K, Ogata N. Macromolecules 1988;21:2997–3003.
[8] Oguchi K, Yoden T, Kosaka Y, Watanabe M, Sanui K, Ogata N. Thin Solid Films 1988;161:305–13.
[9] Yatsue T, Miyashita T. J Phys Chem 1995;99:16047–51.
[10] Aoki A, Abe Y, Miyashita T. Langmuir 1999;15:1463–9.
[11] Hisada K, Ito S, Yamamoto M. Langmuir 1996;12:3682–7.
[12] Mabuchi M, Ito S, Yamamoto M, Miyamoto T, Schmidt A, Knoll W. Macromolecules 1998;31:8802–8.
[13] Ohmori S, Ito S, Yamamoto M. Macromolecules 1990;23:4047–53.
[14] Ohmori S, Ito S, Yamamoto M. Macromolecules 1991;24:2377–84.
[15] Ohmori S, Ito S, Yamamoto M. Macromolecules 1992;25:185–91.
[16] Ohkita H, Ishii H, Ito S, Yamamoto M. Chem Lett 2000:1092–3.
[17] Ohkita H, Ishii H, Ogi T, Ito S, Yamamoto M. Radiat Phys Chem 2001;60:427–32.
[18] Nagai K, Nishijima T, Takamiya N, Tada M, Kaneko M. J Photochem Photobiol A: Chem 1995;92:47–51.
[19] Deisenhofer J, Epp O, Miki K, Huber R, Michel H. Nature 1985;318:618–24.
[20] Wasielewski MR. Chem Rev 1992;92:435–61.
[21] Osuka A, Nakajima S, Okada T, Taniguchi S, Nozaki K, Ohno T, Yamazaki I, Nishimura Y, Mataga N. Angew Chem Int Ed 1996;35:92–5.
[22] Gust D, Moore TA, Moore AL. Acc Chem Res 2001;34:40–8.
[23] Imahori H, Guldi DM, Tamaki K, Yoshida Y, Chuping L, Sakata Y, Fukuzumi S. J Am Chem Soc 2001;123:6617–28.
[24] Nishikata Y, Konishi T, Morikawa A, Kakimoto M, Imai Y. Polym J 1988;20:269–72.
[25] Nishikata Y, Morikawa A, Kakimoto M, Imai Y, Nishiyama K, Fujihira M. Polym J 1990;22:593–600.
[26] Ito S, Kanno K, Ohmori S, Onogi Y, Yamamoto M. Macromolecules 1991;24:659–65.
[27] Sato N, Ito S, Sugiura K, Yamamoto M. J Phys Chem A 1999;103:3402–9.
[28] Shimazaki Y, Mitsuishi M, Ito S, Yamamoto M. Langmuir 1998;14:2768–73.
[29] Hasegawa M, Horie K. Prog Polym Sci 2001;26:259–335.
[30] Hayashi T, Okuyama T, Ito S, Yamamoto M. Macromolecules 1994;27:2270–5.